


RESEARCH ARTICLE | NOVEMBER 21 2023

## Experimental investigation on 15CDV6 austenitic stainless steel and SS321 low alloy steel dissimilar joints by gas tungsten arc welding

B. Indrakanth ; Subramanyam Pavuluri; A. Saravan Bhavan; S. C. Sireesha



AIP Conf. Proc. 2821, 050008 (2023)

<https://doi.org/10.1063/5.0158641>



CrossMark

### AIP Advances

Why Publish With Us?

-  **25 DAYS**  
average time to 1st decision
-  **740+ DOWNLOADS**  
average per article
-  **INCLUSIVE**  
scope

[Learn More](#)



# Experimental Investigation on 15CDV6 Austenitic Stainless Steel and SS321 Low Alloy Steel Dissimilar Joints by Gas Tungsten Arc Welding

B. Indrakanth<sup>a)</sup>, Subramanyam Pavuluri<sup>b)</sup>, A. Saravan Bhavan<sup>c)</sup> and S.C.Sireesha<sup>d)</sup>

Department of Mechanical Engineering, Malla Reddy Engineering College (Autonomous), Maisammaguda, Secunderabad, Telangana -500100, India

<sup>a)</sup>Corresponding author: [birru.indrakanth@gmail.com](mailto:birru.indrakanth@gmail.com)

<sup>b)</sup>[subramanyampavuluri@gmail.com](mailto:subramanyampavuluri@gmail.com)

<sup>c)</sup>[saravanbhavan@gmail.com](mailto:saravanbhavan@gmail.com)

<sup>d)</sup>[sireeshasingapati@gmail.com](mailto:sireeshasingapati@gmail.com)

**Abstract.** Welding using gas tungsten arc (GTAW) is a common method for combining metals that are different or similar in composition. In terms of sound welds, the technique has various benefits. However, the heat input and process speed are still major problems that may be compensated for by sound quality of the resultant welding. The GTAW technique is employed in a variety of industrial applications because of the above-mentioned benefits, including overlay welding, root joint welding, and fill pass welding. It has been discussed in this article how the GTAW technique may be used to fuse dissimilar metals, root joints, and fill pass welding, among other things. The GTAW procedure is used to create dissimilar welds from 15CDV6 stainless steel and SS321 for the study's buttering deposits. Welding chemistry and microstructure are affected by the GTAW process's metallurgical variables. The tensile strength of the GTAW weldment joint is 620, according to the findings of the study. The fractography showed that the GTA weldment had a greater ductility, with an elongation of 26%.

*Keywords:* 15CDV6, SS321, GTAW, Tensile Strength.

## INTRODUCTION

Austenitic stainless steel (15CDV6) and low alloy steel (SS321) have high mechanical, formability, weldability, and corrosion resistance [1,2]. These metal combinations are commonly used in power generation due to their high temperature characteristics [3]. A nuclear water reactor's pressure vessel is joined to stainless steel pipe systems via dissimilar metal welding. It is one of the most sophisticated setups in the recirculation system [4]. Using an austenitic stainless steel filler metal to link two metals with higher carbon content causes carbide to form during welding [5]. Dissimilar weldments [6,7] often fail at the weld due to their inferior structural integrity. Breakdowns in the ferritic-austenitic stainless steel transition zone are typical in fossil-fired steam facilities. Low alloy steel to austenitic stainless welds are less susceptible to stress corrosion cracking. Raman et al. [10] claim that chromium-molybdenum ferritic steel welds may fail in service. Studies are required to prevent similar failures in power plant steam generation/handling systems and petroleum/petrochemical components. Most difficulties arise in the heat affected zone (HAZ) [11–13].

Austenitic steel joints are prone to phase propagation that isn't predicted. Delta ferrite, grain boundary corrosion, and sigma phase are some of the metallurgical changes that occur as a result of this. So welders need to be more efficient. A good illustration of the attention and precautions required is the use of pre- and post-heat treatment methods [14]. There is a micro segregation of Fe, Cr, and C in the interdimeric regions of the weld fusion zone, which results in richer patches. As a result of this segregation, the joints in the dendritic structure lose mechanical properties and corrosion resistance. These difficulties may be avoided or lessened if the welding process and

parameters are appropriately selected. As a result of the above reasons, EBW solidification is less likely to result in the precipitation of undesirable intermetallic components. In the last several years, GTAW has gotten a lot of attention as a way to link metals that otherwise couldn't be joined. According to prior studies, the microstructure of the joints has a significant impact on the mechanical properties of various metals. The study of microstructure and mechanical properties is thus necessary [17]. Roberto [18], Anawa [19], and Olabi [20] studied laser welding of 15CDV6–AISI420 stainless. It's hard to discover research on GTAW welding austenitic stainless to low-alloy steel. The effects of welding processes on different metals have been neglected in the past. This paper describes GTAW welding of different metals. SEM and X-ray diffraction are used to evaluate each weldment's phase composition, microstructure, and mechanical properties (SEM).

## EXPERIMENTAL PROCEDURES

With GTAW Welding Equipment Poared by Inverters Features like pre-setting Amp. metre, soft start, peak and base time for pulse current, pre and post flow of gas, hot start and up and down slope are included in GTAW Welding Machines' features. In order to perform testing, a DCEN GTAW machine is used. All of the parent metals employed in this study, 15CDV6 stainless steel and SS 321 low alloy steel, have been listed in Table.1.



**Figure 1.** GTAW Machine

**Table 1.** Chemical Composition of SS 321

Grade	C	Mn	Si	P	S	Cr	Ni	N
15CDV6	0.12-0.18	0.80-1.10	0.20	0.020	0.015	1.50	-	-
SS321	0.08	2.00	0.75	0.045	0.030	17.0-19.0	9.0-12.0	0.10

**Table 2.** Mechanical Properties of 15CDV6 & SS321 Base Material

S.No.	Yield Strength (MPa) or (N/mm <sup>2</sup> )	Ultimate Tensile Strength (MPa) or (N/mm <sup>2</sup> )	Elongation (%)	Ultimate/ Peak load (kN)
15CDV6	1165.3	1278.9	19.2	38.24
	1031.3	1149.9	20.6	34.60
	1130.2	1253.4	21.7	37.24
SS321	336.9	590.6	52.8	17.72
	335.8	584.3	54.4	17.64
	341.7	589.3	55.2	17.68



**Figure 2.** Weld Specimen

For autogenous weldments, the following parameters are used: Table 2. GTAW specimens are sliced to the desired length. These weld specimens, as well as the metals from which they are made, are sourced from hot forged 6 mm pipe that had been butt-joined for the purposes of GTAW [21-22].

**Table 3.** Welding Parameters Used in this Investigation

Welding Parameters	Units	Range values
Work Distance	mm	275
Purging gas (argon) flow rate	lpm	20
Accelerating Voltage	kV	55
Shielding gas (argon) flow rate	lpm	15
Beam Current (Beam Focus slightly above the Surface)	mA	35-40
Travel Speed	m/min	1
Vacuum Level	mbar	$10^{-4}$

The specimens are cut from the welds and treated as usual to examine the microstructure of the weld. The weld joint featured a Vickers digital micro-hardness tester. The load is applied in seconds. The welded portions are cut up to assess tensile and impact toughness. Wire EDM is utilised to reduce the samples to size while preserving centre weld contact as shown in Figure 3. Scanning Electron Microscopy with EDAX attachment is used to study the shattered morphology of the specimens. Analysis of the phase composition of the joints is done using an XRD equipment [23].

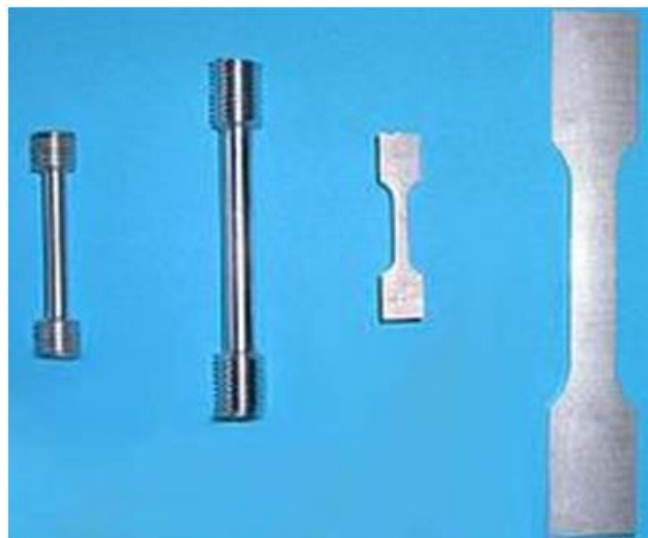


**Figure 3.** Tensile Specimen

## EXPERIMENTAL RESULTS

Scanning Electron Microscopy with EDAX attachment is used to examine the shattered morphology of the specimens. A Philips X-ray diffractometer (XRD) is used to examine the phase composition of the joints under investigation [24].

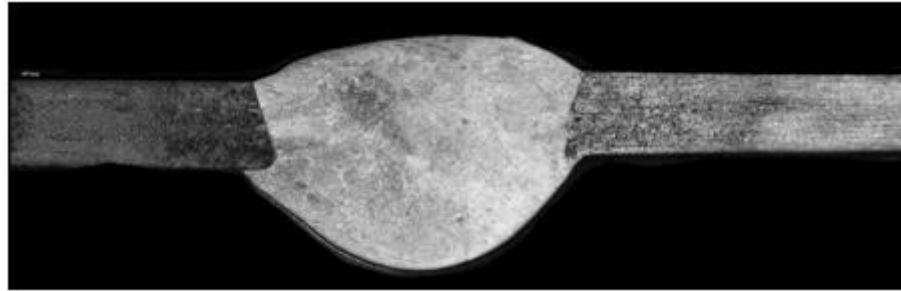


**Figure 4.** Macrostructure of 15CDV6 to SS321 using SS-347 SS filler wire

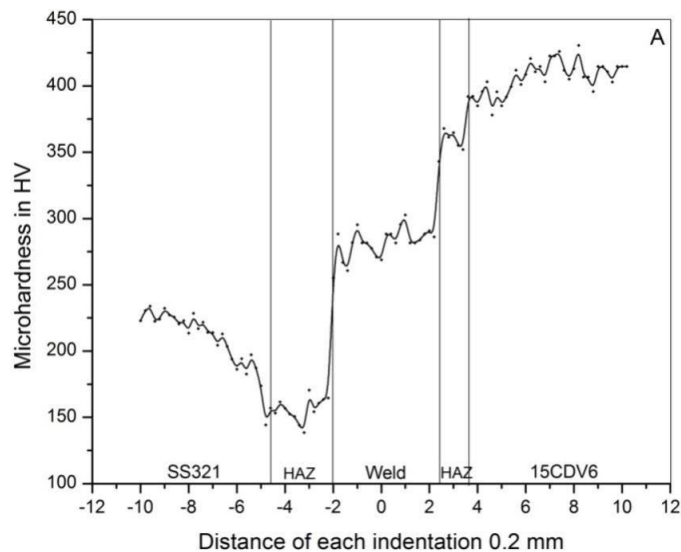
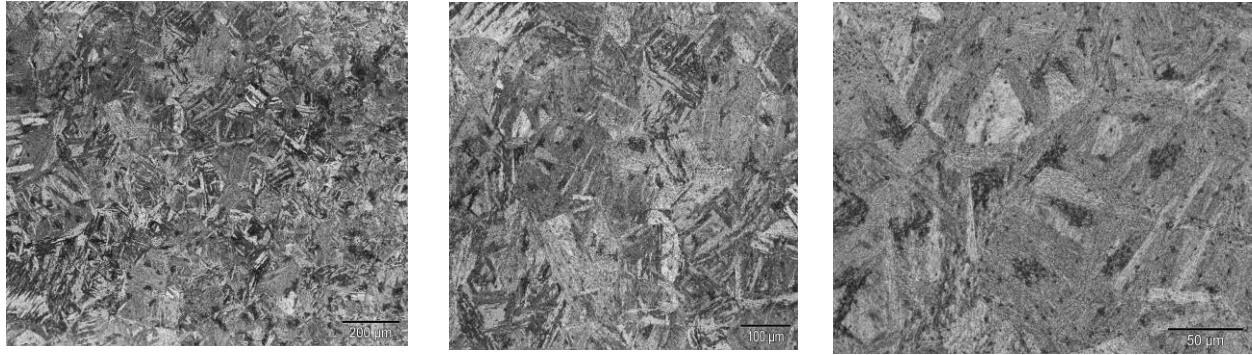


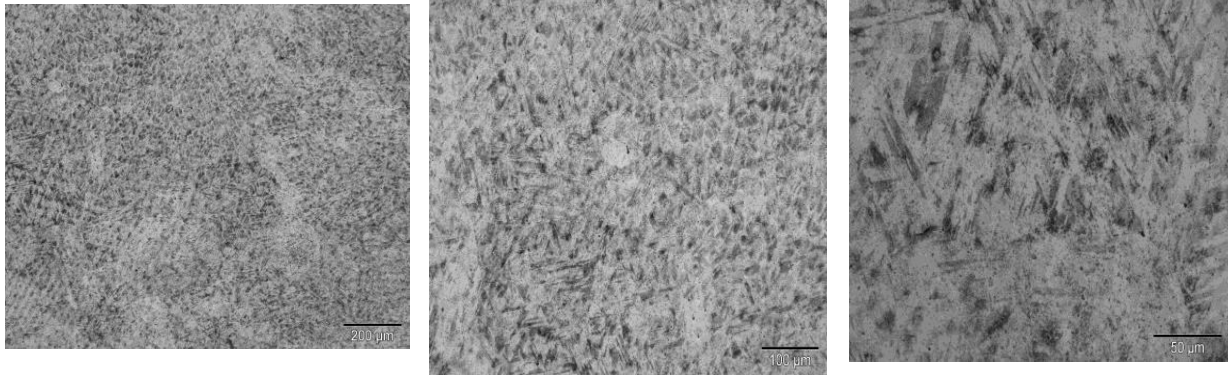
**Figure 5.** Hardness curve welded with SS-347 SS filler wire

SS-321 and 15CDV6 Micro-Hardness of the weld is particularly steady because to the 8CDV12 filler wire utilized. By using this filler wire, the weld's Micro-Hardness may be enhanced. If you look at the XRD data for GTA welded specimens, you'll see that FeNi and Ni<sub>3</sub>C have high intensity peaks whereas the peaks for Cr-Ni-Mo, CrNiFe, Ni<sub>3</sub>C, and other metals are low in intensity [25].

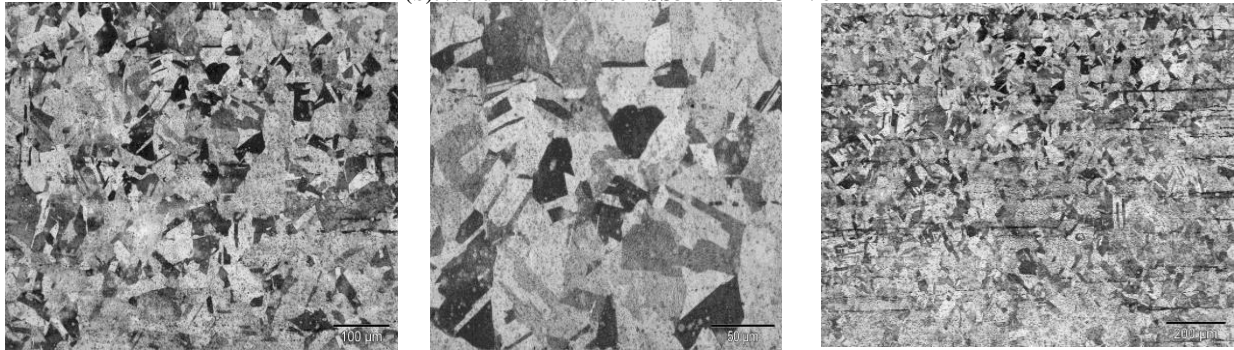
Microstructure of GTA-welded austenitic stainless steel (15CDV6) and low-alloy steel (SS 321) dissimilar weldment is shown in fig.6. Because of the distorted pearlite lamellae present in the low alloy steel, the microstructure of the weld contact has a coarse texture. Around the fusion boundary, some additional directionality has been discovered. During the fusion boundary area, local fluctuations in solidification mode and growth velocity might occur. GTAAW and EBW joints are shown to fuse properly in metallography [26].



(a). coarse heat affected zone of 15cdv6



(b).Weld Zone between SS321 to 15CDV6



(c).Fine Heat Affected Zone of SS321

Figure 6. Microstructures of SS321 to 15CDV6 using SS-347 SS filler wire



Figure 7. Specimen After DP Test



Figure 8. Inspecting of defect after DP test

**Table 4.** Tensile Strength Results

Specimens welded with filler wire	UTS (MPa)	Peak load (kN)	Failure location
15CDV6-SS321 (ER-34755)	620	39	HAZ (SS side)

Table.3 shows the tensile strength of all joints created by the procedures listed above. The average tensile strength of three specimens in each condition has been calculated to assure reproducibility. GTAW has a 620 tensile strength. SEM is used to examine the shattered surface of tensile specimens. Three different welding methods reveal different fracture patterns in joints. GTAW joints are particularly vulnerable to pure-shear fractures, which are the consequence of dislocation slide. The many micro zones shown in Fig. 6 are the subject of this research. Low-alloy steel softens due to decarburization, whereas stainless steel softens due to softening of the substance. As the material's thermal conductivity decreases, heat is trapped. The research found that the increase in hardness at the contact is responsible for both the overall hardness and the soft zone hardness on the low alloy steel side of the interface. Carbon migration from the low alloy steel side to the stainless-steel side is thought to be the cause of this behavior. The hardness of the GTAW weld area ranges from 453 Hv (minimum) to 522 Hv (max).

## DISCUSSIONS

SS321 and 15CDV6 dissimilar welds have extremely low toughness and high hardness, according to a study of their mechanical characteristics. When the GTAW increases, toughness decreases and hardness rises, perhaps as a result of increased carbon migration from low alloy steel to stainless steel. Increasing the breadth of a contact increases friction time, which helps raise the surrounding temperature [22,23]. There is a high correlation between the measured hardness and the findings of other studies [24–26]. The weld interface hardness measured in this research [27].

Carbon depletion may be attributed to the soft zone in low alloy steel, instead of the hard and brittle carbide phases that enrichment in stainless steel creates as has been shown [26]. An intermetallic FeNi/CrNiFe phase formed as a result of the presence of Fe, Ni, and Cr in the weld zone may explain the increased hardness at the interface. This interdiffusion-induced low ductility quassia cleavage fracture is thought to have been caused by the element distribution across the interface and a predominance of fracture characteristics that are mostly cleavage in nature. According to their findings Cheng and Wang found a similar observation. Weldments with smaller widths and lower currents reach lower interface temperatures, lowering the temperature at which metal begins to be extruded, reducing intermetallic formation and carbide precipitation susceptibility. Instead of providing for greater time for precipitation of carbide and intermetallic compounds, the breadth of the welding process and the welding duration increase. As may be seen in Fig. 5, the microhardness curves imply.

The GTAW connection produced a HAZ due to slow welding and high heat input. The outcome is a slower cooling rate and a prolonged hot zone time. Despite its modest size, the fusion pool cools quickly. The decreased mechanical characteristics of the GTAW joint may be due to micro-segregation of alloying elements and the creation of Cr-depleted zones. To increase a material's mechanical qualities, GTAW exposes it to temperatures between 773 and 1073 K.

## CONCLUSION

The following findings may be made as a result of this inquiry. Welding procedures are able to produce good welds between 15CDV6 austenitic stainless steel and SS321 low alloy steel. Filler wires ER-347SS are used to weld 15CDV6 and SS321 together using the TIG method. It is necessary to determine the joint's hardness, microstructure, and tensile preparation. With no faults in the weld zone detected by radiography and Dye penetration testing, the weld is confirmed as successful. In the end, it is determined:

In GTAW weldments, it is found that increasing the width at high-intensity carbide and intermetallic compound current caused brittle fractures. The SEM fractographic of a different GTAW weldment that is impact tested shows fracturing. When different metals are welded together using GTAW, the weld is more durable. The breakdown occurred on the HAZ of SS321, as opposed to the SS321 side weldment, where a GTAW failure is noted. The dissimilar weldment, chromium and nickel diffuse toward SS 321 from 15CDV6 and iron from SS 321 toward

15CDV6 is detected. GTAW welding dissimilar metals results in a greater amount of diffusion. The GTAW weldment has a discrete weld area with chromium, nickel, iron, and carbon enrichment. Due to the superior mechanical qualities of the welded joint, GTAW is well-suited for use in industrial applications when joining 15CDV6 to SS321.

## REFERENCES

1. Rathod, N.J., Chopra, M.K., Chaurasiya, P.K. et al. Optimization on the Turning Process Parameters of SS 304 Using Taguchi and TOPSIS. *Ann. Data. Sci.* (2022). <https://doi.org/10.1007/s40745-021-00369-2>
2. Sakendra Kumar, Satya Prakesh Tewari, Upendra Rajak, Abhishek Dasore, Tikendra Nath Verma, Properties evaluation of A356 and A319 Aluminum alloys under different casting conditions, *Materials Today: Proceedings*, 49(2), 523-528, 2022.
3. Mohammed Anees Sheik, Erdem Cuce, M K Aravindan, Abhishek Dasore, Upendra Rajak, Saboor Shaik, A Muthu Manokar, Saffa Riffat, A comprehensive review on recent advancements in cooling of solar photovoltaic (PV) systems using phase change materials (PCMs), *International Journal of Low-Carbon Technologies*, 2022;, ctac053, <https://doi.org/10.1093/ijlct/ctac053>
4. S.K. Mohammad Shareef, M Sai Vikas, A.L.N Arun Kumar, Abhishek Dasore, Sanjay Chhalotre, Upendra Rajak, Triendra Nath Verma, Design and thermal analysis of engine cylinder fin body using various fin profiles, *Materials Today: Proceedings*, 47(17): 5776-5780 (2021).
5. Surendra, J., Rajyalakshmi, K., Apparao, B. V., Charankumar, G., & Dasore, A. Forecast and trend analysis of gold prices in India using auto regressive integrated moving average model. *J. Math. Comput. Sci.*, 11(2), 1166-1175 (2021).
6. Dasore, A., Rajak, U., Panchal, M. et al. Prediction of Overall Characteristics of a Dual Fuel CI Engine Working on Low-Density Ethanol and Diesel Blends at Varying Compression Ratios. *Arab J Sci Eng* (2022). <https://doi.org/10.1007/s13369-022-06625-8>
7. Nascimento MP, Souza RC, Pigatin WL, Voorwald HJC. Effects of surface treatments on the fatigue strength of AISI 4340 aeronautical steel. *Int J Fatigue* 2001;23:607–18.
8. Arivazhagan N, Singh Surendra, Prakash Satya, Reddy GM. High temperature corrosion studies on friction welded dissimilar metals. *Mater Sci Eng: B J* 2006;132:222–7.
9. Li GF, Charles EA, Congleton J. Effect of post weld heat treatment on stress corrosion cracking of a low alloy steel to stainless steel transition weld. *Corros Sci* 2001;43(10):1963–83.
10. Raman Singh RK, Muddle BC. High temperature oxidation in the context of life assessment and microstructural degradation of weldments of 2.25Cr–1Mo steel. *Int J Press Vess Pip* 2002;79:585–90.
11. Tsay LW, Liu YC, Young MC, Lin DY. Fatigue crack growth of 15CDV6 stainless steel welds in air and hydrogen. *Mater Sci Eng* 2004;A374:204.
12. Johan Singh P, Guha B, Achar DRG. Fatigue life prediction for stainless steel welded CCT geometry based on Larrance's local-stress approach. *Eng Failure Anal* 2003;10:655.
13. Wahap MA, Sakano M. Corrosion and biaxial fatigue of welded structures. *J Mater Process Technol* 2003;410:143–144.
14. Özdemir N, Sarsılmaz F, Haşçalık A. Effect of rotational speed on the interface properties of friction-welded 15CDV6L to 4340 steel. *Mater Des* 2007;28(1):301–307.
15. Lima AS, Nascimento AM, Abreu HFG, de Lima-Neto P. Sensitization evaluation of the austenitic stainless steel AISI304L, 316L, 321 and 347. *J Mater Sci* 2005;40:143.
16. Muthupandi V, Bala Srinivasan P, Seshadri SK, Sundaresan S. Effect of weld metal chemistry and heat input on the structure and properties of duplex stainless steel welds. *Mater Sci Eng A* 2003;358:9–16.
17. Haşçalık A, Ünal E, Özdemir N. Fatigue behaviour of 15CDV6 steel to AISI4340 steel welded by friction welding. *J Mater Sci* 2006;41:3233–9.
18. Roberto Berretta Jose, de Rossi Wagner, Martins das Neves, Mauricio David, de Almeida Ivan Alves, de Rossi Wagner, et al. Pulsed Nd: YAG laser welding of 15CDV6 to AISI 420 stainless steels. *Opt Laser Eng* 2007;45:960–6.
19. Anawa EM, Olabi AG. Optimization of tensile strength of ferritic/austenitic laser-welded components. *Opt Laser Eng* 2008;46:571–7.
20. Rajneesh, N. Srinivasa, et al. "Investigation on mechanical properties of composite for different proportion of natural fibres with epoxy resin." AIP Conference Proceedings. Vol. 2358. No. 1. AIP Publishing LLC, 2021.



21. Pavuluri, Subramanyam, et al. "Effect of reheating cycle on efficiency of Rankine cycle and its practical significance." AIP Conference Proceedings. Vol. 2358. No. 1. AIP Publishing LLC, 2021.
22. Subramanyam Pavuluri, B.Sidda Reddy, B.Durga Prasad, "An Experimental Investigation on the Performance, Combustion and Emission Characteristics of CI Diesel Engine at Various Compression Ratios with Different Ethanol-Biodiesel Blends", International Journal of Advanced Science and Technology, Vol. 29, No.5, pp. 2215-2226, 2020.
23. SanthiPriya, P., Pavuluri, S., Madaria, Y. (2022). Experimental Investigations of Process Variables on Wire Electrical Discharge Machining (WEDM) of AISI 52100 Steel. In: Chaurasiya, P.K., Singh, A., Verma, T.N., Rajak, U. (eds) [Technology Innovation in Mechanical Engineering, Lecture Notes in Mechanical Engineering](#). Springer, Singapore. [https://doi.org/10.1007/978-981-16-7909-4\\_53](https://doi.org/10.1007/978-981-16-7909-4_53)
24. Indrakanth, B., Udaya Bhaskar, S., Ashok Kumar, C., Srinivasa Rajneesh, N. (2022). Design and Optimization of Engine Block Using Gravity Analysis. In: Chaurasiya, P.K., Singh, A., Verma, T.N., Rajak, U. (eds) [Technology Innovation in Mechanical Engineering, Lecture Notes in Mechanical Engineering](#). Springer, Singapore. [https://doi.org/10.1007/978-981-16-7909-4\\_95](https://doi.org/10.1007/978-981-16-7909-4_95)
25. Subramanyam Pavuluri, Dr.B.Sidda Reddy, Dr.B.Durga Prasad. (2020). An Experimental Investigation on the Performance, Combustion and Emission Characteristics of CI Diesel Engine at Various Compression Ratios with Different Ethanol-Biodiesel Blends. International Journal of Advanced Science and Technology, 29(05), 2215-2226. Retrieved from <http://sersc.org/journals/index.php/IJAST/article/view/10988>
26. B. Sidda Reddy, A. Aruna Kumari, J. Suresh Kumar, K. Vijaya Kumar Reddy. Application Of Taguchi and Response Surface Methodology For Biodiesel Production From Alkali Catalysed Transesterification Of Waste Cooking Oil, International Journal of Applied Engineering Research, Vol. 4 (7), pp. 1169–1184, 2009.
27. B. Sidda Reddy, A. V. Hari Babu, S. Sreenivasulu, K. Vijaya Kumar Reddy, Prediction of C. I. Engine Performance and NOX Emission Using CANFIS International Journal of Applied Engineering Research, Vol. 5 (5), pp. 763–778, 2010.